LBL-10226
SLAC-PUB-2758
Preprint

Lawrence Berkeley Laboratory
UNIVERSITY OF CALIFORNIA

Physics, Computer Science & Mathematics Division

Submitted to Physical Review D

RESONANCE PRODUCTION BY TWO-PHOTON INTERACTIONS AT SPEAR

Lawrence Berkeley Laboratory and Department of Physics, University of California, Berkeley, and Stanford Linear Accelerator Center, Stanford University, Stanford, CA

June 1981

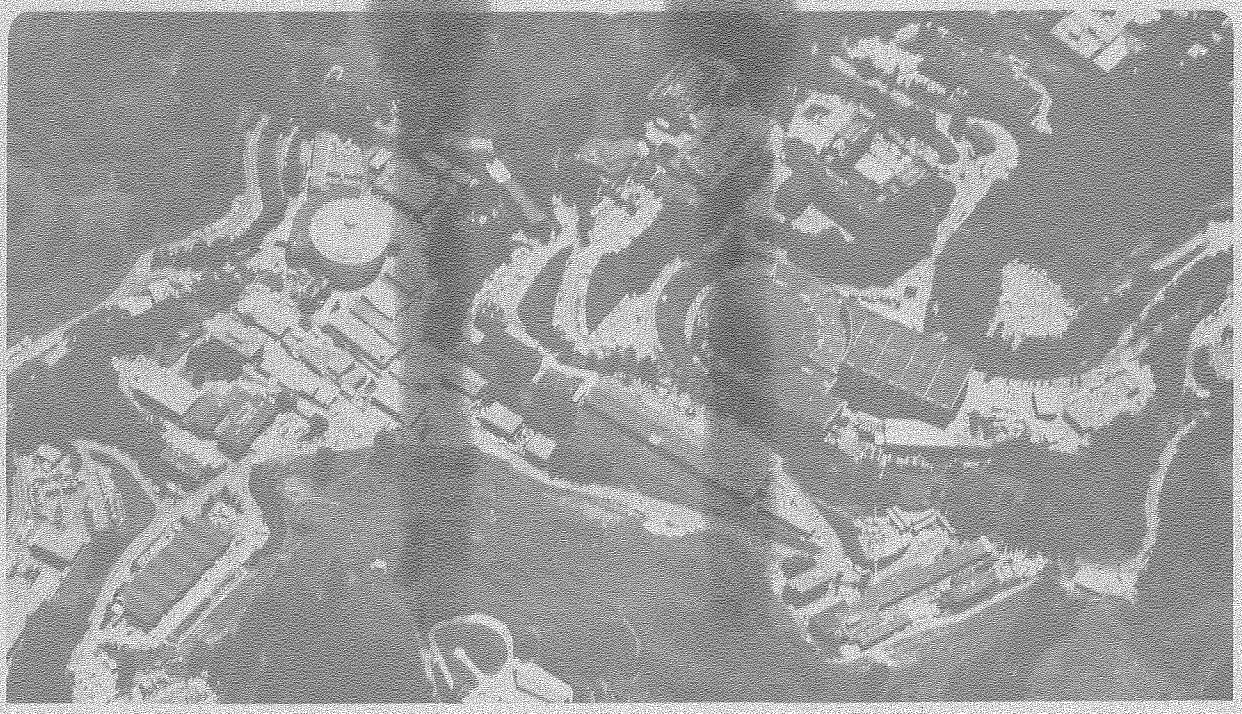

Prepared for the U.S. Department of Energy under Contract DE-AC03-76SF00098

DISCLAIMER

SLAC-PUB-2758
LBL-10226
June 1981
(T/E)

RESONANCE PRODUCTION BY TWO-PHOTON INTERACTIONS AT SPEAR*

P. Jenni,[c] D. L. Burke, V. Telnov,[i] M. S. Alam,[a] A. M. Boyarski, M. Breidenbach, J. Dorenbosch,[c] J. M. Dorfan, G. J. Feldman, M. E. B. Franklin, G. Hanson, K. G. Hayes,[c] T. Himel,[c] D. G. Hitlin,[d] R. J. Hollebeek, W. R. Innes, J. A. Jaros, R. R. Larsen, V. Lüth, M. L. Perl, B. Richter, A. Roussarie,[g] D. L. Scharre, R. H. Schindler,[c] R. F. Schwitters,[e] J. L. Siegrist,[c] H. Taureg,[c] M. Tonutti,[f] R. A. Vidal, J. M. Weiss,[j] and H. Zaccone.[h]
Stanford Linear Accelerator Center
Stanford University, Stanford, California 94305

G. S. Abrams, C. A. Blocker,[e] A. Blondel, W. C. Carithers, W. Chinowsky, M. W. Coles,[b] S. Cooper,[b] W. E. Dieterle, J. B. Dillon, M. W. Eaton, G. Gidal, G. Goldhaber, A. D. Johnson, J. A. Kadyk, A. J. Lankford, M. Levi,[e] R. E. Millikan, M. E. Nelson, C. Y. Pang, J. F. Patrick, J. Strait, G. H. Trilling, E. N. Vella, and I. Videau.[h]
Lawrence Berkeley Laboratory and Department of Physics
University of California, Berkeley, California 94720

ABSTRACT

Two-photon interactions have been studied with the SLAC-LBL Mark II magnetic detector at SPEAR. The cross section for η' production by the reaction $e^+e^- \to e^+e^-\eta'$ has been measured at beam energies from 2.0 GeV to 3.7 GeV. The radiative width $\Gamma_{\gamma\gamma}(\eta')$ has been determined to be 5.8 ± 1.1 keV (±20% systematic uncertainty). Upper limits on the radiative widths of the f(1270), A_2(1310) and f'(1515) tensor mesons have been determined. A search has been made for production of the E(1420) by $\gamma\gamma$ collisions, but no signal is observed.

(Submitted to Physical Review D)

* Work supported in part by the Department of Energy, contracts DE-AC03-76SF00515 and W-7405-ENG-48, by the Universität Bonn, Federal Republic of Germany, the centre d'Études Nucléaires de Saclay, France, and the Miller Institute for Basic Research in Science, Berkeley, CA.
Present Addresses:
a Vanderbilt University, Nashville, TN 37235.
b DESY, Hamburg, Federal Republic of Germany.
c EP Division, CERN, Geneva, Switzerland.
d California Institute of Technology, Pasadena, CA 91125.
e Harvard University, Cambridge, MA 02138.
f Universität Bonn, Federal Republic of Germany.
g CEN-Saclay, France.
h LPNHE, École Polytechnique, Palaiseau, France.
i Inst. of Nuclear Physics, Novosibirsk, 90, USSR.
j Argonne National Laboratory, 9700 S. Cass Ave., Argonne, IL 60439.

I. INTRODUCTION

The observation of leptons and hadrons produced by two-photon interactions in electron-positron colliding beam experiments has been a challenge ever since the importance of the two-photon mechanism was pointed out over ten years ago.[1-3] The basic diagram for the two-photon process is shown in Fig. 1. Evidence for the production of lepton pairs by collisions of two photons has been reported by several groups,[3-8] but until recently only a few events with hadrons in the final state were observed.[7,9] The first evidence of a meson resonance produced by the two-photon interaction was reported by the SLAC-LBL Mark II collaboration;[10] the reaction

$$e^+e^- \to e^+e^-\eta'(958) \qquad (1)$$

was observed by detecting the $\eta' \to \pi^+\pi^-\gamma$ final state. Extensive studies of production of hadronic resonances by the gamma-gamma process are now being reported.[11-18]

In this article we present the results of searches for meson resonances produced in two-photon processes. The corresponding cross sections are directly proportional to the radiative widths $\Gamma_{\gamma\gamma}(X)$ of the resonances X as first pointed out by Low.[19] We have used this relation to determine the radiative width $\Gamma_{\gamma\gamma}(\eta')$ of the $\eta'(958)$ meson to be 5.8 ± 1.1 keV (±20% systematic uncertainty) from a measurement of reaction (1). The cross section for reaction (1) is observed to increase over the beam energy range covered by this experiment, 1.95 GeV to 3.70 GeV, as expected for two-photon processes.[1-3] Our result is in good agreement with predictions from models with fractionally charged quarks[20-22] under assumptions[21] which will be mentioned later.

After a short description of the SLAC-LBL Mark II magnetic detector we present in Section III of this paper our results on reaction (1) including all data accumulated at the Stanford Linear Accelerator Center e^+e^- storage ring facility SPEAR with beam energies E_b above 1.95 GeV. These data represent an increase in integrated luminosity of about a factor 3 over our previously published data sample.[10] In Section IV we present results of searches for two-photon production of the following final states: $A_2(1310) \to \rho^{\pm}\pi^{\mp}$, $f(1270)$, $A_2(1310)$ or $f'(1515)$ decaying into K^+K^-, and $E(1420) \to K^oK^{\pm}\pi^{\mp}$. No signal has been found and upper limits on the radiative width of these resonances are given.

II. THE MARK II DETECTOR

A schematic view of the SLAC-LBL Mark II Magnetic detector is shown in Fig. 2. Its configuration and performance have been described elsewhere.[10,23] The detector consists of a large cylindrical drift chamber surrounded by time-of-flight (TOF) scintillation counters. These are both embedded in a solenoidal magnet. Liquid argon electromagnetic shower calorimeters (LA) and a muon detection system are located outside of the magnet coil. Additional shower counters cover both ends of the cylindrical detector.

The performance features may be summarized as follows. The aximuthal coordinates for charged tracks are measured in the drift chamber to a rms accuracy of about 210 μm per layer. The magnetic field is 4.1 kG, and when tracks are constrained to pass through the known beam position the momenta of charged particles are determined with a resolution $\delta p/p = \pm\left[(0.005p)^2 + (0.0145)^2\right]^{\frac{1}{2}}$ where p is the momentum in GeV/c. The resolution of the time-of-flight system is 300 ps rms for hadrons. This provides one standard deviation separation of π from K at momenta of 1.35 GeV/c, and a similar separation of K from p at 2.0 GeV/c. The rms energy resolution for photons and electrons in the liquid argon calorimeter has been measured to be $\delta E/E = 0.11/\sqrt{E}$ (E in GeV) at high energies ($E \gtrsim 0.5$ GeV). The resolution is slightly poorer ($0.13/\sqrt{E}$) at lower energies because of the increased importance of the energy loss in the 1.36 radiation lengths of material (coil and supports) in front of the calorimeter. The rms angular resolution for low energy photons is about 8 mrad both in azimuth and dip angle. The measured photon detection efficiencies are 15% at 100 MeV, 50% at 200 MeV and ≥90% above 400 MeV, exclusive of geometry. The LA detector is also used for electron-pion separation. Pion misidentification probabilities of less than 4% and electron efficiencies above 77% are achieved for particle momenta greater than 500 MeV/c. This performance improves at higher momenta. Finally, muons are detected above p ~ 700 MeV/c with proportional tubes embedded in a segmented steel hadron absorber. The fraction of the full solid angle covered by the drift chamber and the TOF counters is 75%, by the LA detector is 65%, and by the muon detection system is 55%.

A two stage hardware trigger[24] was used to select, with efficiency ≥99%, all interactions with at least one charged particle at $|\cos\theta_L| < 0.75$ and transverse momentum $p_\perp > 100$ MeV/c, and another particle with $|\cos\theta_L| \lesssim 0.85$.

III. MEASUREMENT OF THE TWO-PHOTON PRODUCTION OF THE η'

First results on reaction (1) have been previously reported by the SLAC-LBL Mark II experiment.[10] In the following analysis we used the same method with similar event selection criteria. All data accumulated at beam energies E_b above 1.95 GeV were used; the results presented here include the previously published data sample.

The events sought were $\eta' \to \pi^+\pi^-\gamma$ decays where no additional final state particles were detected. The outgoing e^+ and e^- in reaction (1) were not detected. Therefore, events were selected which have only two oppositely charged tracks coming from the interaction region and one photon measured in the LA detector.

The charged particles were identified as pions if their TOF was within 3 standard deviations of the expected time, they deposited less energy in the LA than that expected for electrons, and there were no track-associated hits in the muon chambers behind the hadron absorber. Only those events with an invariant $\pi^+\pi^-$ pair mass of less than 1 GeV/c^2, with each pion momentum less than 1 GeV/c, and with a photon energy E_γ within $0.180 < E_\gamma < 1.0$ GeV were considered further. With the lower photon energy cut we removed background generated by electronic noise fluctuations (spurious photons).

Kinematical cuts were then applied to reduce the contributions from the two principal background sources. Possible backgrounds from one photon e^+e^- annihilation events with some of the final state particles not detected were suppressed by requiring that the transverse momentum $p_\perp$ of the $\pi^+\pi^-\gamma$ state be less than 250 MeV/c and that the acoplanarity angle $\Delta\phi$ between the $\pi^+\pi^-$ and the γ momentum vectors projected into a plane

perpendicular to the beam axis be less than 20° ($\Delta\phi = 0^\circ$ for back-to-back decays). The background from lepton or pion pairs produced in two-photon interactions combined with noise-generated spurious photons was suppressed by requiring that the transverse momentum of the $\pi^+\pi^-$ state be larger than 50 MeV/c and that the acoplanarity angle between the two pions be larger than 3°.

The $\pi^+\pi^-\gamma$ invariant mass distribution $m_{\pi^+\pi^-\gamma}$ for the events which satisfy all the selection criteria is shown in Fig. 3(a). There is a clear signal of events from the decay $\eta' \to \pi^+\pi^-\gamma$. The observed rms width of about 40 MeV/c for the η' mass signal is mostly due to the photon energy resolution and agrees well with a Monte Carlo calculation. The shift of the η' signal by ~25 MeV/c^2 towards higher masses is caused by the steep rise of the photon detection efficiency as a function of the deposited energy in the LA for energies below 400 MeV. This mass shift can be investigated experimentally in the following way. Resonances produced in two-photon interactions at SPEAR energies occur mainly at very low transverse momenta $p_\perp$ with respect to the axis of the colliding electron beams. This fact can be exploited by constraining the events to zero net $p_\perp$ and using a calculated photon energy instead of the measured one. This procedure reduces the expected mass resolution for the η' signal to about 15 MeV/c^2 (rms) and removes the mass shift. However, for events with an η' produced with non-zero $p_\perp$ it gives an incorrect mass value. The mass distribution with the constraint $p_\perp = 0$ is shown in Fig. 3(b) for the η' region and displays the expected features.

The only explicit cut applied on the dipion mass was $m_{\pi\pi} < 1$ GeV/c^2. We find that the dipion mass distribution for the events in the η' mass

region, defined as $900 < m_{\pi\pi\gamma} < 1050$ MeV/c^2, is compatible with the hypothesis that all pairs in the $\eta' \to \pi^+\pi^-\gamma$ signal come from ρ^o decays.

The kinematics of two-photon reactions are very characteristic and different from other processes. For the η' produced by reaction (1) the kinematics are distinct from those of mesons in multi-hadron events from one photon e^+e^- annihilation reactions. The transverse momentum $p_\perp$ distribution is shown in Fig. 4 for all the data (full histogram) and for the subsample of events lying in the η' mass region (shaded). The η' mesons have lower $p_\perp$ than the background events. The distribution of the total energy E is shown in Fig. 5. The energy of the η' appears to be confined to low values, excluding the possibility that the η' is produced in a two-body annihilation reaction like $\eta'\gamma$ with the γ not detected. The angular distribution of the η' mesons is strongly peaked along the beams. Their rapidity (y) distribution, given in Fig. 6, is flat over the whole detector acceptance of about $-0.5 < y < 0.5$, whereas the background events tend to peak around $y = 0$.

The background was studied with two different methods. In the first method we analyzed multihadron e^+e^- annihilation events. The same analysis cuts as for reaction (1) except for the topology selection were applied to events with three or more charged prongs and at least one photon. The resulting mass distribution is smooth and reaches a broad maximum over the range from 0.8 to 1.3 GeV/c^2. The transverse momentum distribution rises below about 125 MeV/c and stays approximately constant above. In the second method we used all the original selection criteria including the exclusive topology of two-charged prongs and only one photon, but then combined the dipion state from one event with the photon from

the next event. This analysis reproduces the shape and the normalization of the observed background in the mass and transverse momentum distributions. Both these studies suggest a smooth background shape under the η' signal, and we have therefore made a direct subtraction using the adjacent mass regions. (See Table I.) This subtraction makes no specific assumptions about the origin of the background. The background contribution is lower for the data taken at the higher beam energies than for the low energy part of the data. (See Fig. 3(a).)

The cross section was calculated using the branching ratio $B(\eta' \to \pi^+\pi^-\gamma) = 0.298 \pm 0.017$[25] and the detection efficiency ε (see Table I) determined by a Monte Carlo simulation. Events were generated according to the cross section calculation and angular distribution of Ref. 26. These events were then subject to the same detector geometry and selection criteria as the real data except for the LA shower cuts on the charged tracks. Because of the difficulties of describing in detail the interaction of pions in the shower counter material, the efficiencies of the latter cuts (typically 85%) were determined experimentally with unambigously identified pions from ψ decays. Furthermore, there is a small (5%) loss of events due to additional spurious photons which was also determined experimentally. The observed cross section $\sigma(\eta')$ is given in Table I. The cross section $\sigma(\eta')$ is also displayed in Fig. 7 as a function of the beam energy and is compatible with the expected slow rise with increasing energy. The errors shown are statistical only and do not include an estimated overall systematic uncertainty of ±20%. The principal contributions to this value come from uncertainty in the model dependence of the photon spectrum in the Monte Carlo

calculation (±15%), the photon detection efficiency in the LA (±10%), the experimentally measured losses due to the LA cuts on the charged tracks (±5%), and the integrated luminosity (±6%). We did not correct the displayed cross sections for initial state radiation in reaction (1).

The two-photon production cross section for a resonance X is directly proportional to the radiative width $\Gamma_{\gamma\gamma}(X)$ of the resonance.[19] For example, in the equivalent photon approximation calculation of Ref. 2, the cross section for the production of a narrow resonance is given by:

$$\sigma_{ee \to eeX} = 16\alpha^2 \cdot \frac{(2J+1)}{m_X^3} \cdot \Gamma_{\gamma\gamma}(X) \cdot \left(\ln \frac{E_b}{m_e} - \frac{1}{2} \right)^2 \cdot f\left(\frac{m_X}{2E_b} \right) \quad (2)$$

with

$$f(\xi) = \left(2+\xi^2\right)^2 \ln \frac{1}{\xi} - \left(1-\xi^2\right)\left(3+\xi^2\right) \quad .$$

J denotes the spin and m_X the mass of the resonance. E_b is the beam energy and m_e the electron mass. From the measured cross section for reaction (1) we determined $\Gamma_{\gamma\gamma}(\eta') = 5.8 \pm 1.1$ keV (±20% systematic uncertainty) using the two-photon calculation of Ref. 26. In this calculation we included the correction for initial state radiation effects. Upper limits on $\Gamma_{\gamma\gamma}(\eta')$ in the range 11 to 35 keV were obtained in other searches[6,7,9] for reaction (1) and values of 5.4 ± 1.0 keV and 5.0 ± 0.5 keV have recently been reported[16] from PETRA. From the radiative width we deduced the total width $\Gamma_{tot}(\eta') = 293 \pm 67$ keV or equivalently the mean life $\tau(\eta') = (2.2 \pm 0.5) \times 10^{-21}$ sec (±20% systematic uncertainty) using the branching fraction $B(\eta' \to \gamma\gamma) = 0.0197 \pm 0.0026$.[25] This measurement of $\Gamma_{tot}(\eta')$ is in good agreement with the value 280 ± 100 keV reported in Ref. 27.

The radiative width for the η' was calculated by several authors.[20-22] Quark models with fractionally charged quarks lead, under the assumptions of a small pseudoscalar octet-singlet mixing angle and of equal singlet and octet decay constants, to the prediction of $\Gamma_{\gamma\gamma}(\eta') \simeq 6$ keV in very good agreement with our measurement. Applying the same assumptions, the data are not compatible with integral charge quark models, for which a radiative decay width of about 26 keV was predicted. However, the validity of these assumptions was questioned in Ref. 21 where alternative analyses are proposed.

IV. THE TENSOR MESONS f, A_2, AND f' AND THE E(1420)

We investigated exclusive final states for the following reactions:

$$e^+e^- \to e^+e^- A_2(1310) \to \rho^{\pm}\pi^{\mp} \quad (3)$$

$$e^+e^- \to e^+e^- f(1270) \to K^+K^- \quad (4)$$

$$e^+e^- \to e^+e^- A_2(1310) \to K^+K^- \quad (5)$$

$$e^+e^- \to e^+e^- f'(1515) \to K^+K^- \quad (6)$$

$$e^+e^- \to e^+e^- E(1420) \to K^0K^{\pm}\pi^{\mp} \quad (7)$$

by searching for signals in the invariant mass distributions of the respective final states at low transverse momenta. As in the measurement

of reaction (1), the final state e^+ and e^- remained undetected. No signal above background was detected for any of these states. We used the data taken at beam energies above 2.25 GeV (14 pb^{-1} integrated luminosity) to determine upper limits on the radiative widths of these mesons on the basis of these reactions.

A. $\rho^{\pm}\pi^{\mp}$ Final State

To search for reaction (3), we used events with two oppositely charged pions and two photons. Candidate A_2 events were required to contain two photons, each in the energy range $0.1 < E_\gamma < 1.0$ GeV, and an invariant mass $m_{\gamma\gamma}$ within $0.075 < m_{\gamma\gamma} < 0.200$ GeV/c^2. For these events the photon energies were adjusted to constrain $m_{\gamma\gamma}$ to m_{π^0}. These π^0 were combined with each of the charged pions to form the invariant mass $m_{\pi^{\pm}\pi^0}$. Only those events with a $\rho^{\pm}$ candidate, defined as $0.5 < m_{\pi^{\pm}\pi^0} < 1.0$ GeV/c^2, were retained any further. Special cuts were necessary to suppress the background from τ lepton pair production. Tau decays into $\rho^{\pm}\nu_\tau$ and final states containing single or multipions were measured in the same experiment.[28] To remove this background, both the $\rho^{\pm}$ and the $\pi^{\mp}$ momenta were required to be less than 800 MeV/c. Finally, the invariant $\rho^{\pm}\pi^{\mp}$ mass was formed, and a transverse momentum cut of $p_\perp < 250$ MeV/c was applied to reduce the background from one photon e^+e^- annihilation events. The $m_{\rho^{\pm}\pi^{\mp}}$ and $p_\perp$ distributions are shown in Figs. 8(a) and 8(b), with the events lying in the A_2 mass region $1.20 < m_{\rho^{\pm}\pi^{\mp}} < 1.45$ GeV/c^2 shaded in Fig. 8(b). From the observed background in the $m_{\rho^{\pm}\pi^{\mp}}$ distribution, the known $B(A_2 \to \rho^{\pm}\pi^{\mp}) = 0.703 \pm 0.021$,[25] and the overall detection efficiency for reaction (4) $\varepsilon = 0.0028$, which is greatly reduced due to the low energy

photon efficiency, one deduces a 95% C.L. upper limit for $\sigma(A_2) < 0.36$ nb at $E_b = 2.85$ GeV for reaction (3). From Eq. (2) it follows that $\Gamma_{\gamma\gamma}(A_2) < 2.5$ keV. A possible systematic error of 25% was included in these limits. Values of $\Gamma_{\gamma\gamma}(A_2)$ of 0.77 ± 0.18 and 0.59 ± 0.14 have been reported respectively by the Crystal Ball[15] and CELLO[16] groups.

B. K^+K^- Final State

The K^+K^- decay modes of the f(1270), A_2(1310), and f'(1515) mesons can be used to study their two-photon production with little background from one photon e^+e^- annihilation processes. For this purpose we selected events with only two oppositely charged prongs and no detected photons. Both tracks were required to be identified as kaons by the TOF measurement. This was achieved by a cut on the probability level[29] which was required to be larger than 0.65 for each of the two tracks to be kaons. In order to reduce sources other than two-photon production we applied two loose kinematical cuts: the acoplanarity angle $\Delta\phi$ between the two kaons had to be $<20^\circ$ and the $p_\perp$ of the K^+K^- state had to be <250 MeV/c. The invariant mass $m_{K^+K^-}$ and the $p_\perp$ distributions are given in Figs. 9(a) and 9(b). The $p_\perp$ of most of the events is seen to be very small as expected for reactions (4) to (6).

Nonresonant production can also contribute to the K^+K^- final state from two-photon interactions. We estimated the contribution to the $m_{K^+K^-}$ distribution from the nonresonant process

$$e^+e^- \to e^+e^-K^+K^- \qquad (8)$$

with the equivalent photon approximation of Ref. 30. The curve in Fig. 9(a) shows the result of using a simple Φ pole for the kaon form factor.

With this assumption the contribution of reaction (8) appears to be small (10% over the range of observed K^+K^- masses). Interpretation of the observed spectrum is complicated, however, by the large background of pion pairs produced by the two-photon mechanism.[13] The structure seen near 1.5 GeV/c^2, for example, is consistent with a small (~1%) misidentification of $\gamma\gamma \to f(1270) \to \pi^+\pi^-$ events. We, therefore, only give upper limits on the production cross sections for the f(1270) and $A_2(1310)$ mesons in reactions (4) and (5). We use branching ratios[25] into K^+K^- of 0.0165 ± 0.0020 and 0.0235 ± 0.0025 and overall detection efficiencies of 0.0167 and 0.0172, respectively, at the average beam energy of 2.85 GeV. The cross section results, as well as the upper limits on $\Gamma_{\gamma\gamma}$ from Eq. (2), are given in Table II. The branching ratio of the f'(1515) meson into $K\bar{K}$ is not known, but expected to be dominant[25] [i.e., $B(f' \to K^+K^-)$ near 0.5]. The data together with the calculated detection efficiency of 0.0195 provide therefore only upper limits on $B(f' \to K^+K^-) \times \sigma(f')$ and $B(f' \to K^+K^-) \times \Gamma_{\gamma\gamma}(f')$ for reaction (6). These upper limits are also listed in Table II. A systematic uncertainty for the K^+K^- final state of 15% was included in the listed 95% C.L. upper limits.

We summarized in Table II the upper limits on the radiative widths of the f(1270), $A_2(1310)$, and f'(1515) mesons obtained from reactions (3) to (6). These limits are compatible with reported[11-16] values of the f(1270) and $A_2(1310)$ widths and the assignment of these three mesons to an ideally mixed SU(3) multiplet.

C. $K^oK^\pm\pi^\mp$ Final State

We have previously reported[31] observation of a $K\bar{K}\pi$ resonance in prompt-photon decays of the $\psi(3095)$ that we tenatively identified as the E(1420) meson. The spin assignment of this meson is uncertain with both $J^P = 0^-$ and 1^+ having been reported (see Ref. 31 and references therein). More recent analyses[32] of decays of the ψ indicate that there may, in fact, be two distinct resonances with masses near 1420 MeV/c^2 that produce the $K\bar{K}\pi$ final state. Observation of appreciable production of a state in this mass region by untagged two-photon collisions would establish the 0^- assignment for that state.

We have searched for $K\bar{K}\pi$ final states by selecting four-prong events with zero total charge and low net transverse momentum, $|\sum \vec{p}_T| \leq 0.250$ GeV/c. One of the four prongs was required to be identified as a charged kaon by TOF (probability level larger than 0.5), and a K^o candidate was required to be formed by one of the two remaining $\pi^+\pi^-$ pair combinations ($0.478 < m_{\pi\pi} < 0.518$). The invariant mass spectrum of all events that satisfy these criteria is given in Fig. 10. We see one event within three half-widths of the resonant mass, and hence, to be conservative, we calculate a limit based on this event. The detection efficiency for this state was computed by Monte Carlo to be $\varepsilon = 0.0056$. To compute this value it was assumed that the decay of the E to $K\bar{K}\pi$ proceeds via an intermediate $\delta(980)\pi$ state. If the $K\bar{K}\pi$ decay channel is assumed to proceed by pure phase space, then a larger efficiency is obtained. Since our data from the $\psi(3095)$ heavily favor the $\delta\pi$ mode and since this mode gives the lower detection efficiency, we use the quoted efficiency to compute the limit $\Gamma_{E(1420) \to \gamma\gamma} \cdot BR_{E \to K\bar{K}\pi} < 8.0$ keV (95% C.L.). A

factor of three has been included in this value to account for the fraction of all $K\bar{K}\pi$ decays that result in $K_S^o K^{\pm}\pi^{\mp}$, and the spin of the resonance was assumed to zero.

V. SUMMARY

We have studied meson resonance production by the two-photon interaction in a e^+e^- colliding beam experiment. We observe exclusive events containing no particle in the detector other than an $\eta'(958)$ detected in the decay mode $\eta' \to \pi^+\pi^-\gamma$. On the basis of kinematics these events are interpreted as coming from the reaction $e^+e^- \to e^+e^-\eta'$ where the final state e^+ and e^- are not detected. As expected for two-photon processes, the cross section for these events is observed to rise as the beam energy increases from 1.95 to 3.7 GeV. From the observed cross section the radiative width of the η' meson $\Gamma_{\gamma\gamma}(\eta')$ is determined to be 5.8 ± 1.1 keV (±20% systematic uncertainty). This value is in good agreement with (model dependent) predictions from various quark models with fractionally charged quarks, and excludes, within these models, the possibility of integral charge quarks.

We have also investigated the two-photon production of the tensor mesons f(1270), $A_2(1310)$, and f'(1515) by searching for signals in the mass distributions of various exclusive final states. The $K^oK^{\pm}\pi^{\mp}$ mass spectrum was examined for evidence of the E(1420) meson that has been observed in prompt photon decays of the $\psi(3095)$. No signals were observed in any of these channels, and upper limits on the radiative widths of these resonances have been given.

ACKNOWLEDGEMENTS

We wish to thank Drs. S. J. Brodsky and F. J. Gilman for stimulating discussions. This work was supported in part by the Department of Energy, contracts DE-AC03-76SF00515 and W-7405-ENG-48, by the Universität Bonn, Federal Republic of Germany, the centre d'Études Nucléaires de Saclay, France, and the Miller Institute for Basic Research in Science, Berkeley, California.

REFERENCES

1. N. Arteaga-Romero, A. Jaccarini and P. Kessler, C. R. Acad. Sci. B269, 153 (1969) and B269, 1129 (1969); N. Arteaga-Romero, A. Jaccarini, P. Kessler and J. Parisi, Nuovo Cimento Lett. 4, 933 (1970) and Phys. Rev. D3, 1569 (1971).
2. S. J. Brodsky, T. Kinoshita and H. Terazawa, Phys. Rev. Lett. 25, 972 (1970) and Phys. Rev. D4, 1532 (1971).
3. V. E. Balakin, V. M. Budnev and I. F. Ginsburg, Zh. Eksp. Teor. Fiz. Pis´ma Red. 11, 559 (1970) [Soviet Phys. JETP Lett. 11, 388 (1970)].
4. V. E. Balakin et al., Phys. Lett. 34B, 663 (1971); C. Bacci et al., Nuovo Cimento Lett. 3, 709 (1972); G. Barbiellini et al., Phys. Rev. Lett. 32, 385 (1974).
5. A. Courau et al., Phys. Lett. 84B, 145 (1979).
6. H. J. Besch et al., Phys. Lett. 81B, 79 (1979).
7. R. Baldini Celio et al., Phys. Lett. 86B, 239 (1979).
8. D. P. Barber et al., Phys. Rev. Lett. 43, 1915 (1979).
9. S. Orito et al., Phys. Lett. 48B, 380 (1974); L. Paoluzi et al., Nuovo Cimento Lett. 10, 435 (1974).
10. G. S. Abrams et al., Phys. Rev. Lett. 43, 477 (1979).
11. PLUTO Collaboration, Ch. Berger et al., Phys. Lett. 94B, 254 (1980).
12. C. J. Biddick et al., Phys. Lett. 97B, 320 (1980).
13. A. Roussarie et al., Phys. Lett. 105B, 304 (1981).
14. TASSO Collaboration, R. Brandelik et al., Z. Phys. C. - Particles and Fields, 10, 117 (1981).
15. C. Edwards et al., SLAC-PUB-2821 (1981).

16. JADE Collaboration, W. Bartel et al., Phys. Lett. 113B, 190 (1982). CELLO Collaboration, H. J. Behrend et al., DESY 82-008 (1982).
17. D. L. Burke, Proceedings of Fourth International Conference on Photon-Photon Interactions, Paris, 1981, ed. by G. W. London.
18. E. Hilger, Proceedings of Fourth International Conference on Photon-Photon Interactions, Paris, 1981, ed. by G. W. London.
19. F. E. Low, Phys. Rev. 120, 582 (1960).
20. S. Matsuda and S. Oneda, Phys. Rev. 187, 2107 (1969); S. Okubo, in "Symmetries and Quark Models," R. Chand, ed., Gordon and Breach, New York (1970); H. Suura, T. F. Walsh and B.-L. Young, Nuovo Cimento Lett. 4, 505 (1972).
21. M. S. Chanowitz, Phys. Rev. Lett. 35, 977 (1975) and Lawrence Berkeley Laboratory preprint LBL-9639 (1979).
22. E. Etim and M. Greco, Nuovo Cimento 42, 124 (1977); N. M. Chase and M. T. Vaughn, Z. Phys. C2, 23 (1979).
23. W. Davies-White et al., Nucl. Instrum. Methods 160, 227 (1979); G. S. Abrams et al., IEEE Trans. on Nucl. Sci. NS-25, 309 (1978). G. S. Abrams et al., IEEE Trans. on Nucl. Sci. NS-27, 59 (1980).
24. H. Brafman et al., IEEE Trans. on Nucl. Sci. NS-25, 692 (1978).
25. Compiled by Particle Data Group, Phys. Lett. 75B, 1 (1978).
26. V. M. Budnev and I. F. Ginzburg, Phys. Lett. 37B, 320 (1971); V. N. Baier and V. S. Fadin, Nuovo Cimento Lett. 1, 481 (1971), and private communication.
27. D. M. Binnie et al., Phys. Lett. 83B, 141 (1979).
28. G. S. Abrams et al., Phys. Rev. Lett. 43, 1555 (1979).

29. Each track is assigned weights for being a pion, kaon or proton. Each weight is proportional to the probability that if the particle has the assumed identity, its flight time would have the measured value. The normalization is such that the sum of all weights for a given track is unity.

30. S. J. Brodsky, Suppl. J. Phys., tome 35, page C2-69 (1974) and Ref. 2.

31. D. L. Scharre et al., Phys. Lett. 97B, 329 (1980).

32. See D. L. Scharre, SLAC-PUB-2880, talk at Orbis Scientiae 1982, Miami Beach, Florida (1982).

TABLE I

Summary of the cross section calculation. E_b is the beam energy, $\int \mathscr{L} dt$ is the integrated luminosity, ε is the detection efficiency not including $B(\eta' \to \pi\pi\gamma)$, $n_{\eta'}$ is the background subtracted number of η' events and $\sigma(\eta')$ is the observed cross section. Only statistical errors are shown; the overall systematic uncertainty is ±20%.

E_b (GeV)	$\int \mathscr{L} dt$ (nb^{-1})	ε	$n_{\eta'}$	$\sigma(\eta')$ (nb)
1.95-2.21	4199	0.0231	7.7 ± 5.1	0.27 ± 0.18
2.25-2.50	2131	0.0224	4.3 ± 2.6	0.30 ± 0.18
2.50-3.00	6655	0.0211	25.9 ± 7.1	0.62 ± 0.17
3.00-3.35	4009	0.0177	20.0 ± 5.9	0.94 ± 0.28
3.70	984	0.0125	3.1 ± 2.2	0.84 ± 0.60

TABLE II

Upper limits (95% C.L.) on the two-photon production cross section σ and the radiative width $\Gamma_{\gamma\gamma}$ of the tensor mesons at the luminosity weighted average beam energy 2.85 GeV. The overall detection efficiency is listed under ε and B stands for branching ratio.

Final State	Meson	ε	σ (nb)	$\Gamma_{\gamma\gamma}$ (KeV)
$\rho^{\pm}\pi^{\mp}$	$A_2(1310)$	0.0028	< 0.36	< 2.5
K^+K^-	$f(1270)$	0.0167	< 4.2	< 24.0
K^+K^-	$A_2(1310)$	0.0172	< 2.6	< 17.0
K^+K^-	$f'(1515)$	0.0195	$\sigma \times B(f' \to K^+K^-)$ < 0.052	$\Gamma_{\gamma\gamma} \times B(f' \to K^+K^-)$ < 0.6
$K^0K^{\pm}\pi^{\mp}$	$E(1420)$	0.0056		$\Gamma_{\gamma\gamma} \times B(E \to K\bar{K}\pi)$ < 8.0

FIGURE CAPTIONS

1. Diagram for the two-photon production of the state X.
2. Schematic view of the Mark II detector. (A) vacuum chamber, (B) pipe counter, (C) drift chamber, (D) time-of-flight counters, (E) solenoid coil, (F) liquid argon shower counters, (G) iron absorber, and (H) muon proportional tubes.
3. (a) $\pi^+\pi^-\gamma$ invariant mass distribution. Events from beam energies equal or above 2.6 GeV are shown shaded. (b) $\pi^+\pi^-\gamma$ invariant mass distribution with $p_\perp = 0$ constraint.
4. Transverse momentum distribution. Events in the η' peak $0.90 < m_{\pi^+\pi^-\gamma} < 1.05$ GeV/c^2 are shaded.
5. Total energy distribution. Events in the η' peak $0.90 < m_{\pi^+\pi^-\gamma} < 1.05$ GeV/c^2 are shaded.
6. Rapidity distribution for the $\pi^+\pi^-\gamma$ states, with the events in the η' peak shaded.
7. Cross section for $e^+e^- \to e^+e^-\eta'$ as a function of the beam energy. The curve is the result of Eq. (2) with $\Gamma_{\gamma\gamma}(\eta') = 6$ keV.
8. (a) $\rho^{\pm}\pi^{\mp}$ invariant mass distribution. (b) Transverse momentum distribution; events from the $A_2(1310)$ mass region $1.20 < m_{\rho^{\pm}\pi^{\mp}} < 1.45$ GeV/c^2 are shaded.
9. (a) Invariant K^+K^- mass distribution. The curve shows the expected contribution from nonresonant two-photon interactions (see text). (b) Transverse momentum distribution of the K^+K^- system.
10. The observed $K^0K^{\pm}\pi^{\mp}$ invariant mass spectrum for events with $|\sum \vec{p}_T| < 0.250$ GeV/c.

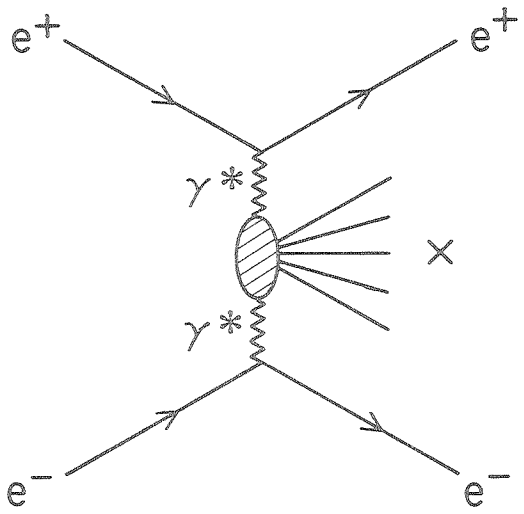

Fig. 1

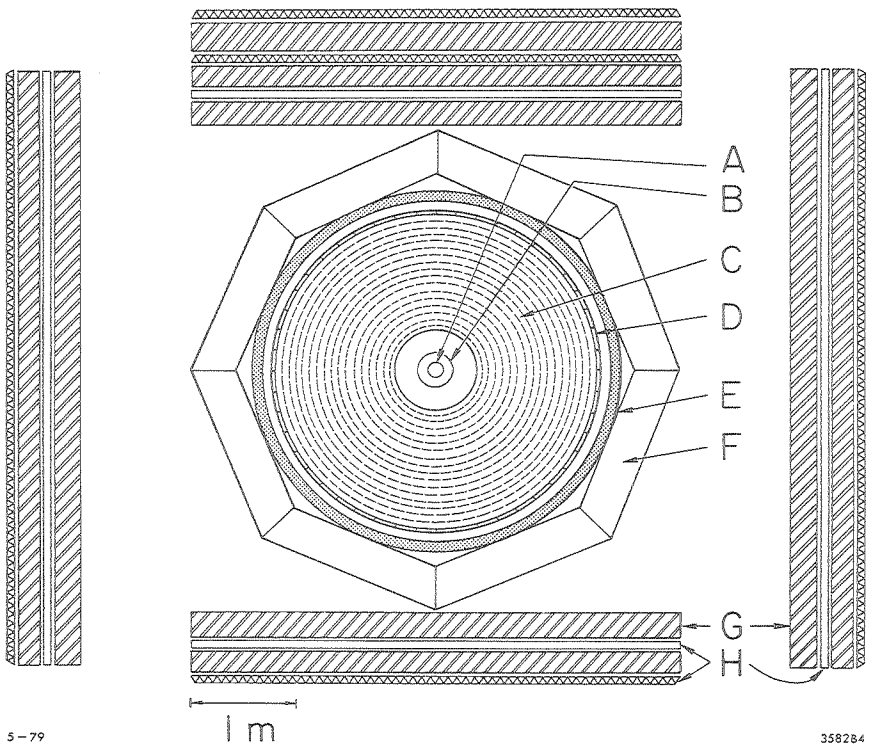

Fig. 2

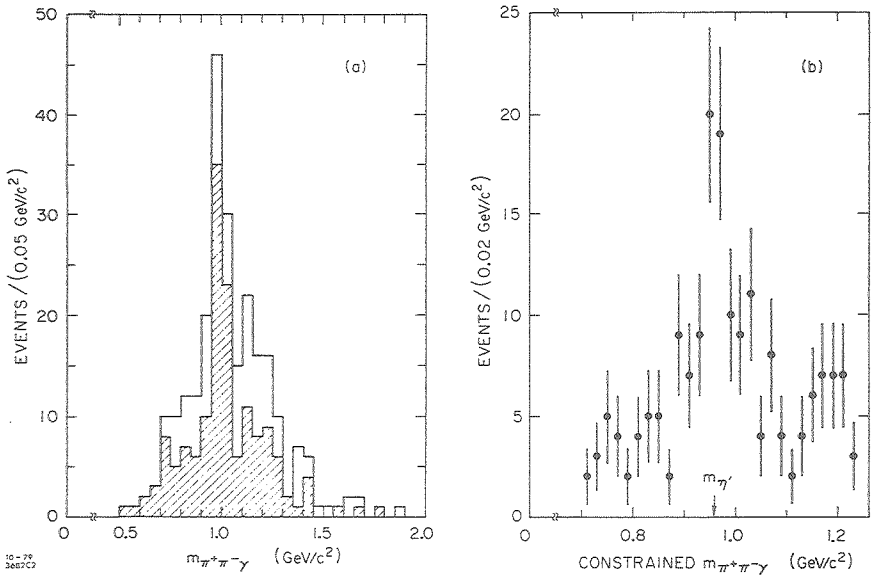
(a)
(b)
EVENTS/(0.05 GeV/c²)
EVENTS/(0.02 GeV/c²)
$m_{\pi^+\pi^-\gamma}$ (GeV/c²)
CONSTRAINED $m_{\pi^+\pi^-\gamma}$ (GeV/c²)
$m_{\eta'}$

Fig. 3

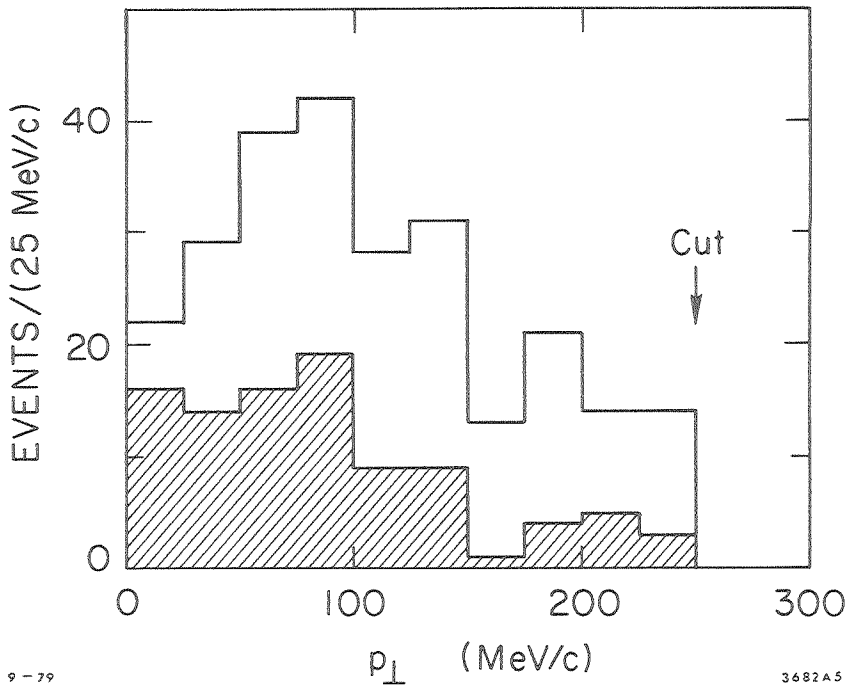
EVENTS/(25 MeV/c)
Cut
$p_\perp$ (MeV/c)
9-79
3682A5

Fig. 4

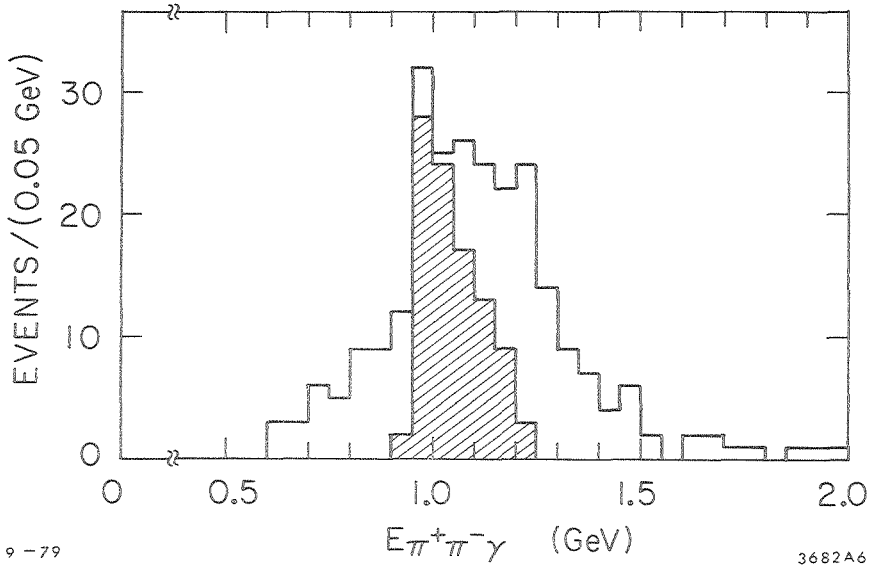
EVENTS/(0.05 GeV)
30
20
10
0
0
0.5
1.0
1.5
2.0
$E_{\pi^+\pi^-\gamma}$ (GeV)
9-79
3682A6

Fig. 5

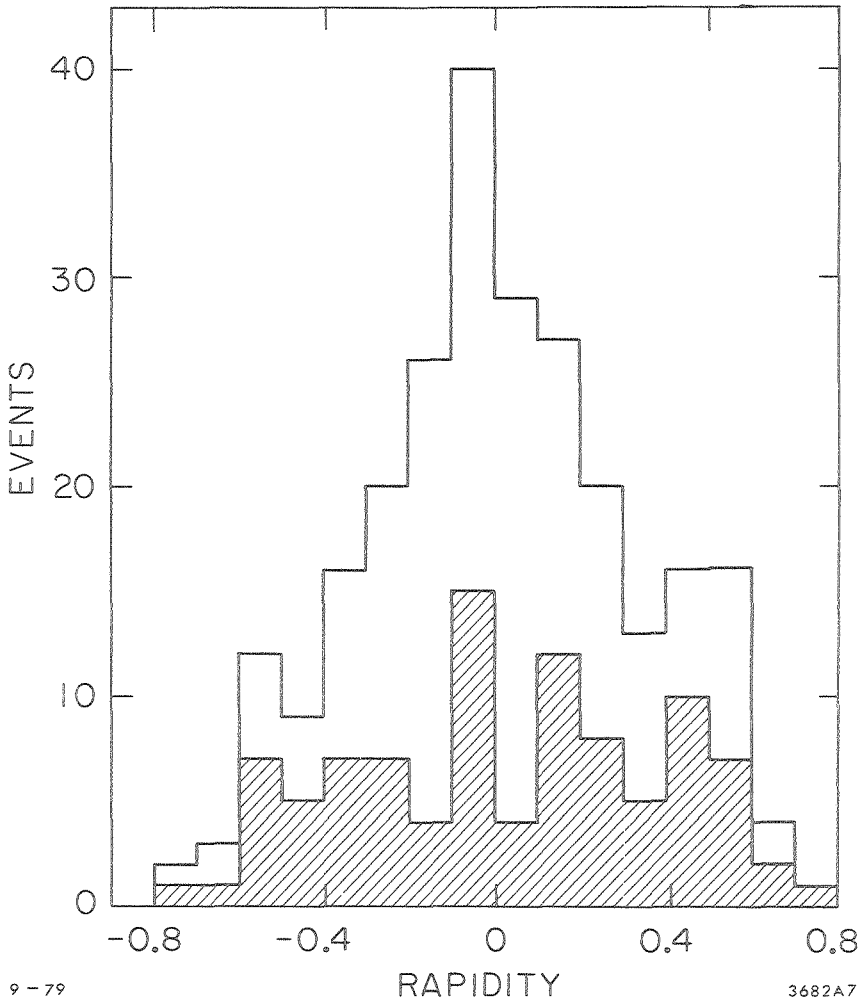
EVENTS
40
30
20
10
0
-0.8
-0.4
0
0.4
0.8
RAPIDITY
9-79
3682A7

Fig. 6

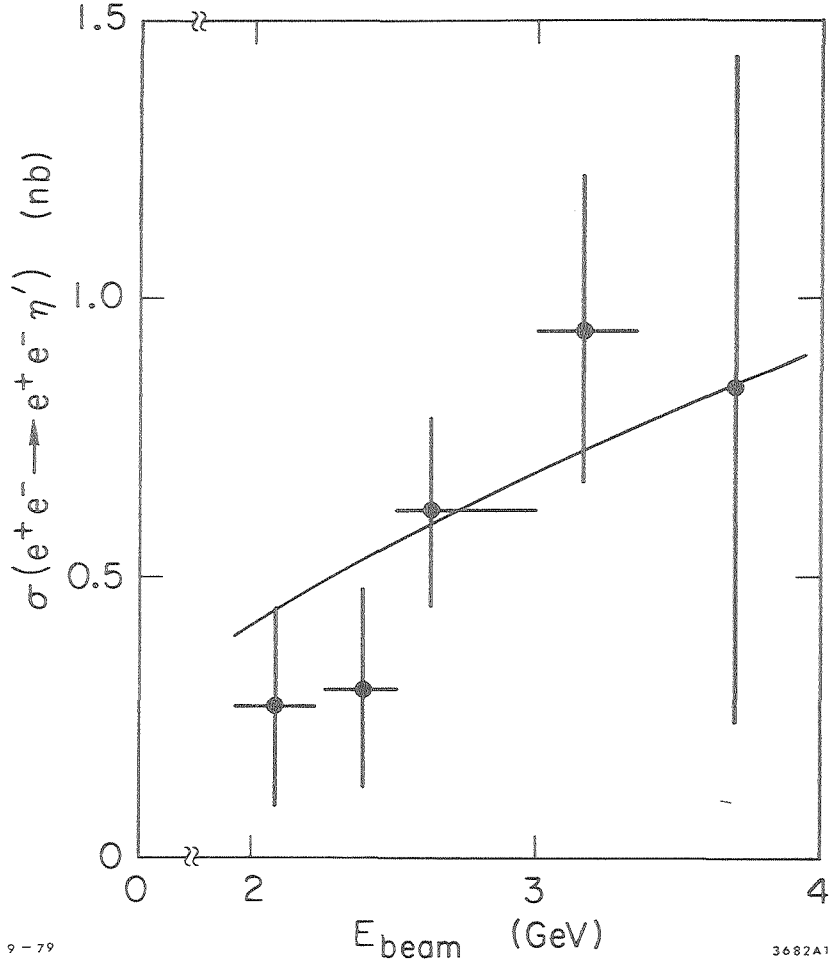
1.5
1.0
0.5
0
0
2
3
4
$\sigma(e^+e^- \rightarrow e^+e^-\eta')$ (nb)
E_{beam} (GeV)
9-79
3682A1

Fig. 7

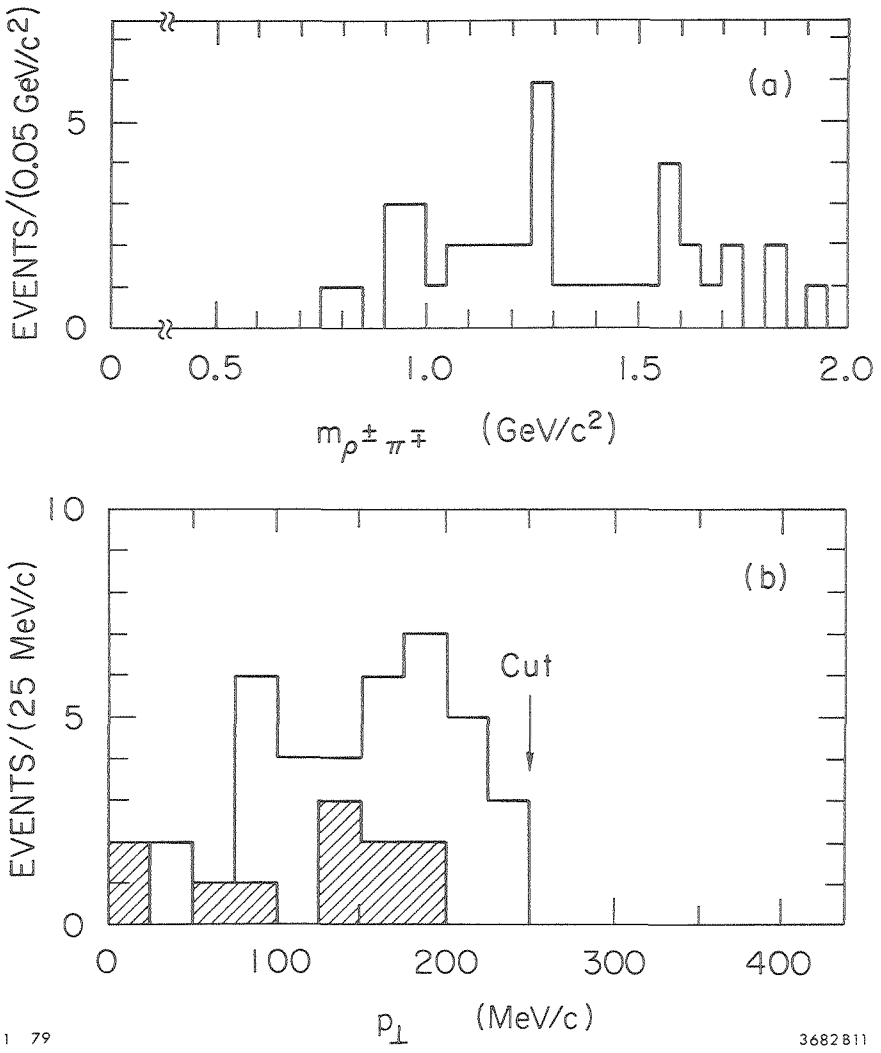
(a)
EVENTS/(0.05 GeV/c²)
5
0
0
0.5
1.0
1.5
2.0
$m_{\rho^\pm\pi^\mp}$ (GeV/c²)
(b)
EVENTS/(25 MeV/c)
10
5
0
Cut
0
100
200
300
400
$p_\perp$ (MeV/c)
11 79
3682B11

Fig. 8

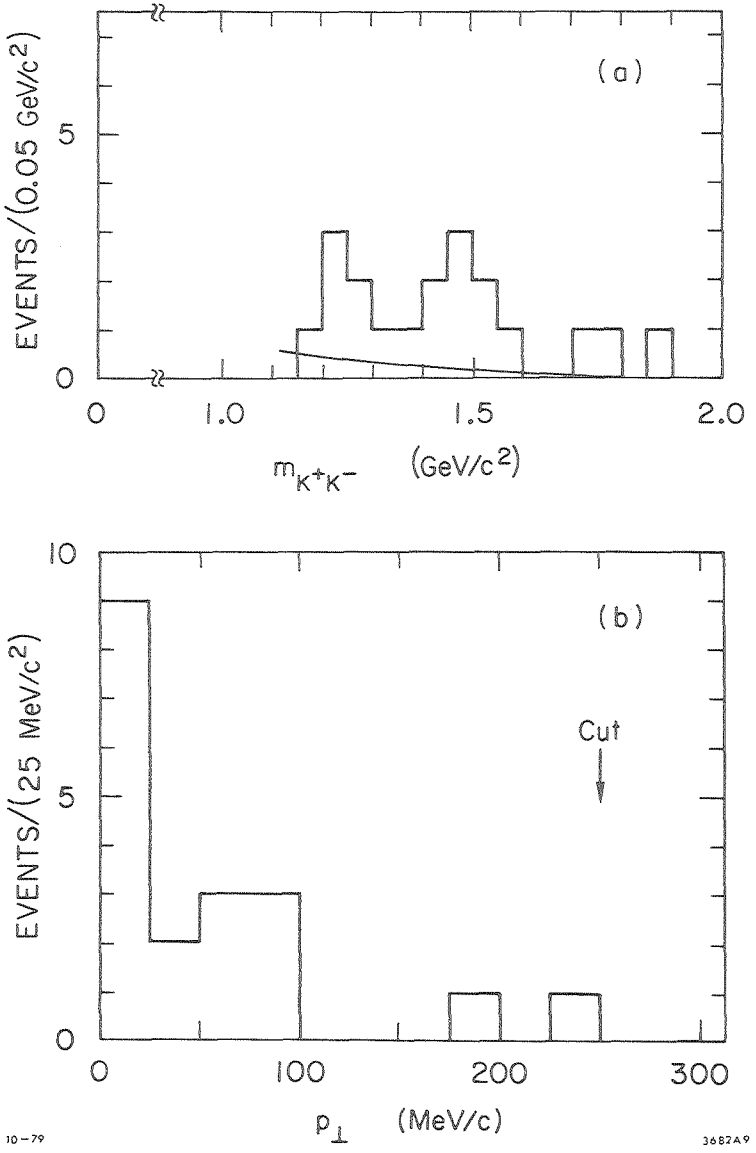
(a)
EVENTS/(0.05 GeV/c²)
5
0
0
1.0
1.5
2.0
m K⁺K⁻ (GeV/c²)
10
(b)
Cut
EVENTS/(25 MeV/c²)
5
0
0
100
200
300
p⊥ (MeV/c)
10-79
3682A9

Fig. 9

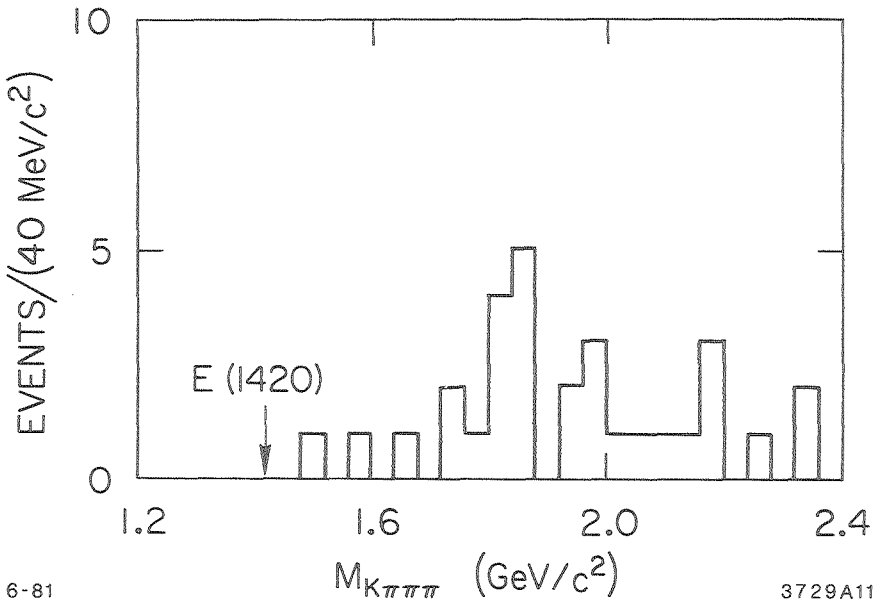
10
EVENTS/(40 MeV/c²)
5
0
E (1420)
1.2
1.6
2.0
2.4
M Kπππ (GeV/c²)
6-81
3729A11

Fig. 10